JOURNAL OF AGRICULTURAL AND FOOD CHEMISTRY

ARTICLE

pubs.acs.org/JAFC

Identification of Hen Egg Yolk-Derived Phosvitin Phosphopeptides and Their Effects on Gene Expression Profiling against Oxidative Stress-Induced Caco-2 Cells

Denise Young,[†] Françoise Nau,[‡] Maryvonne Pasco,[‡] and Yoshinori Mine*[,†]

[†]Department of Food Science, University of Guelph, Guelph, Ontario N1G 2W1, Canada

[‡]UMR 1253 INRA-Agrocampus Rennes Sciences et Technologie du Lait et de l'Oeuf, 65 rue de Saint Brieuc, 35042 Rennes Cedex, France

ABSTRACT: Oxidative stress is involved in the initiation and propagation of chronic intestinal pathologies. Bioactive peptides such as egg yolk-derived phosvitin phosphopeptides (PPP3) have been previously shown to reduce in vitro oxidative stress by up-regulating glutathione synthesis and antioxidant enzyme activities. Peptide and gene expression profile analysis of the PPP3 peptides can provide insight into structures involved in signal transduction mechanisms in the antioxidative stress response. The objectives of this research were to identify the PPP3 amino acid sequences before and after simulated gastrointestinal digestion and to assess the genes influenced by PPP3. Peptide sequences were analyzed using ESI Q-TOF-MS/MS, and the expression profile of 84 human oxidative stress and antioxidant defense genes were analyzed. Undigested PPP3 was composed of three main peptides: GTEPDAKTSSSSSASSTATSSSSSSASSPNRKKPMDE (phosvitin-PV residues 4−41), NSKSSSSSSKSSSSSSRSRSSSKSSSSSSSSSSSSSSKSSSSR (PV residues 155−197), and EDDSSSSSSSSVLSKIWGRHEIYQ (PV residues 244−257) and their fragments. There was limited degradation of PPP3 after gastrointestinal digestion as deduced from the fragment sizes of digested PPP3, which ranged from 5 to 32 amino acids. These fragments were rich in contiguous serines and, in some cases, monoesterified with phosphate. Both undigested and digested PPP3 significantly reduced IL-8 secretion in H_2O_2-induced Caco-2 cells, indicating that antioxidative stress bioactivity is retained upon digestion. After PPP3 pretreatment, antioxidant genes associated with oxygen and reactive oxygen species (ROS) metabolism and cellular responses to chemical stimulus, oxidative stress, and ROS are up-regulated in the presence and absence of oxidative stress, thereby contributing to the prevention of intestinal oxidative stress and the promotion of gut health.

KEYWORDS: oxidative stress, phosvitin, phosphopeptides, mass spectrometry, PCR array, gene ontology, bioinformatics

INTRODUCTION

An imbalance of reactive oxygen species (ROS) to antioxidants and oxidant detoxification systems can lead to oxidative stress and cellular damage. In the gastrointestinal tract, prolonged duration of high levels of oxidative stress could lead to the development or persistence of chronic conditions such as inflammatory bowel diseases, ischemic-reperfusion disorders, and intestinal cancer.[1] Vitamin C, vitamin E, and endogenous antioxidants such as glutathione (GSH) and antioxidative stress enzymes such as catalase (CAT), superoxide dismutase (SOD), glutathione peroxidase (GPx), glutathione reductase (GR), and glutathione-*S*-transferase (GST) often act together to reduce oxidants and re-establish a stable redox balance. Although endogenous antioxidant mechanisms are triggered naturally in response to oxidative stress, some food-derived compounds have been shown to (1) further up-regulate glutathione synthesis by increasing the gene expression and activity of γ-glutamylcysteine synthetase (γ-GCS), (2) elevate GSH concentrations, and (3) increase the activities of antioxidative enzymes.[2−5] The transcription of these genes is often linked to the nuclear response factor 2−antioxidant response element (Nrf2-ARE) pathway,[6] which is dependent on the release of Nrf2 from the cytosol, subsequent nuclear translocation, and binding to ARE in the promoter region of antioxidant genes.

Peptides isolated from phosvitin, a highly phosphorylated egg yolk protein with >50% serine residues, are found to exhibit a range of antioxidative stress properties. A bioactive fraction of phosvitin phosphopeptides, PPP3, reduced proinflammatory interleukin-8 (IL-8) secretion, lowered lipid peroxidation by-products, increased intracellular GSH levels and γ-GCS mRNA activity, and elevated CAT, GR, and GST activities in H_2O_2-induced Caco-2 intestinal cell culture.[7,8] PPP3 is the third fraction of an anion-separated phosvitin hydrolysate, which was prepared by the alkaline hydrolysis and tryptic digestion of phosvitin.[7] Of the three chromatographic separations, PPP3 was composed of the highest phosphorus and serine percentages of 18.9% (w/w) and possessed the highest bioactivity. Interestingly, phosvitin, *o*-phosphoserine, and dephosphorylated phosvitin peptides did not reduce IL-8 during in vitro oxidative stress.[7] The PPP3 amino acid composition was determined, but provides limited insight on the peptide sequence and whether bioactivity is maintained after gastrointestinal digestion.

Received: May 25, 2011
Revised: July 29, 2011
Accepted: July 29, 2011
Published: July 29, 2011

Table 1. Peptides Identified in Undigested PPP3 Using Nano-LC-MS/MS Mass Spectrometry[a]

Position	Sequence	Observed (m/z)	Mr (expt)	Mr (calc)	Modification
1115-1151	GTEPDAKTSSSSSSASSTATSSSSSSASSPNRKKPMD	1230.2019	3687.5839	3687.569	
1115-1152	GTEPDAKTSSSSSSASSTATSSSSSSASSPNRKKPMDE (PV residue 4-40(41))	1267.8816	3800.6231	3800.6167	
1216-1258	NSKSSSSSSKSSSSSSRSRSSSKSSSSSSSSSSSSSSKSSSSR (PV residue 155-197)	1100.7112	4398.8157	4398.7566	3 Phospho (STY)
1305-1323	EDDSSSSSSSSVLSKIWGR	1007.4728	2012.931	2012.9287	
1305-1325	EDDSSSSSSSSVLSKIWGRHE	760.6952	2279.0636	2279.0302	
1305-1326	EDDSSSSSSSSVLSKIWGRHEI	798.3963	2392.167	2392.1142	
1305-1328	EDDSSSSSSSSVLSKIWGRHEIYQ (PV residue 244-257)	895.431	2683.2713	2683.2361	
1307-1325	DSSSSSSSSVLSKIWGRHE	1018.5105	2035.0065	2034.9606	
1308-1325	SSSSSSSSVLSKIWGRHE	1000.9581	1999.9017	1999.9	Phospho (STY)
1318-1325	SKIWGRHE	506.7848	1011.555	1011.525	
1318-1326	SKIWGRHEI	563.3258	1124.637	1124.609	
1318-1327	SKIWGRHEIY	644.8508	1287.6871	1287.6724	
1318-1328	SKIWGRHEIYQ	708.8829	1415.7513	1415.7309	

[a] PPP3 was dephosphorylated prior to LC-MS/MS. Observed *m/z* values are obtained by mass spectrometry. Mr(expt) is the uncharged molecular mass of the peptide, and Mr(calc) is the theoretical mass of the closest matching peptide.

Phosvitin is resistant to gastrointestinal (GI) proteolysis[9] partly due to the abundance of phosphate moieties. In the native protein, phosphate groups are largely monoesterified to serine and are arranged in blocks of up to 15 consecutive residues.[10] PPP3, similar to most dietary proteins and peptides, is likely to undergo drastic structural changes during ingestion, digestion, and absorption. Proteinases such as pepsin, trypsin, and chymotrypsin in the gastrointestinal tract and brush-border peptidases at the surface of epithelial cells hydrolyze peptides to smaller increments.[11] Therefore, the PPP3 peptide sequence and substrate specificities of the digestive enzymes will invariably influence the fragment sizes and the peptide's functionality. In this study, we identify the peptides in undigested and pepsin- and pancreatin-digested PPP3 and assess the effect of PPP3 on an array of antioxidant and oxidant genes expressed during oxidative stress.

MATERIALS AND METHODS

Materials. All reagents were purchased from Sigma-Aldrich Co. (St. Louis, MO) unless otherwise specified.

PPP3 Preparation Method. The PPP3 fraction was isolated from the crude phosvitin phosphopeptide (PPPs) mixture using anion-exchange high-performance liquid chromatography (HPLC) according to the procedure of Katayama et al.[8] Briefly, PPPs were injected into a Mono Q HR 5/5 anion exchange column (Pharmacia Biotech, Uppsala, Sweden) and eluted with 20 mM ammonium bicarbonate with a linear NaCl gradient from 0 to 1.0 M. Three fractions were collected, and the last fraction, PPP3, was subsequently dialyzed using a 500 kDa MWCO membrane (Spectrum Laboratories Inc., Rancho Dominguez, CA) and freeze-dried.

Simulated Gastrointestinal Digestion of PPP3. Human digestion of PPP3 was simulated in vitro using pepsin and pancreatin. To prepare the digested PPP3, PPP3 (5 mg) was first dissolved in 100 μL of 0.15 N HCl (pH 1.5). Porcine pepsin (EC 3.4.23.1, 3210 U/mg protein, Sigma-Aldrich) was added at an enzyme/substrate ratio of 1:250 (w/w), and the mixture were incubated at 37 °C for 2 h. KH_2PO_4 (50 μL, 0.5 M) and pancreatin (Sigma-Aldrich) at an enzyme/substrate ratio of 1:50 (w/w) were incorporated, and the solution was incubated at 37 °C for 8 h at pH 8.0. The digestion was terminated by heating at 90 °C for 5 min.

PPP3 Dephosphorylation. PPP3 and digested PPP3 were combined with phosphatase (E:S = 1:25) prepared in a 10 mM potassium acetate/acetic acid buffer (pH 5.2) and incubated for 8 h at 37 °C. After incubation, the enzyme was inactivated at 80 °C for 10 min. Free phosphates and salts in the dephosphorylated samples were removed by dialysis for two consecutive days with daily changes of water using a 500 Da cutoff membrane (Spectrum Laboratories Inc.). Samples were then freeze-dried and rehydrated just prior to mass spectrometry analysis.

Peptide Identification by ESI Q-TOF-MS/MS. Native and digested PPP3 peptide sequence analysis was performed at the mass spectrometry facility, Institut National Supérieur de Formation Agro-alimentaire (INSFA, Agrocampus Rennes, Rennes, France). All mass spectra of intact oligopeptides were obtained using matrix-assisted laser ionization/desorption time-of-flight (MALDI-TOF) configuration with a Voyager DE STR spectrometer (Applied Biosystem, Courtaboeuf, France) equipped with a nitrogen laser (337 nm, 20 Hz). All nanoelectrospray mass spectrometry (nES-MS) experiments for peptide mapping were conducted on a Q-TOF hybrid quadrupole/time-of-flight instrument (Micromass, Manchester, U.K.), for high resolution and online liquid chromatography−tandem mass spectrometry (LC-MS/MS) analyses. An external calibration was first performed in the range of 500−3000 Da. The monoisotopic mass lists were compared to the proteomic server (http://us.expasy.org/) using Protein prospector software (http://prospector.ucsf.edu/) for peptide mass fingerprinting (PMF) analysis. The list of peptide masses was searched against the nonredundant protein sequence database provided by the National Center for Biotechnology Information (NCBI) server (http://www.ncbi.nlm.nih.gov).

Cell Culture. The Caco-2 human intestinal cell line (American Type Culture Collection, Rockville, MD) was used in all in vitro oxidative stress studies. Cells were grown in Dulbecco's modified Eagle's medium/F12 (DMEM/F12; Gibco, Burlington, ON, Canada) supplemented with 20% fetal bovine serum (FBS; Hyclone, Logan, UT) and 50 units/mL of penicillin−streptomycin (Gibco) and were incubated at 37 °C in a 5% CO_2 chamber. Cell passages 15−45 were used to form the confluent monolayers required for the in vitro experiments. Monolayers were formed from 2×10^5 cells, which were grown for 5−7 days with fresh medium replacements every 2−3 days.

Evaluation of Antioxidative Stress Activity in Vitro. Confluent Caco-2 cells in 48-well culture plates (Corning Costar, Cambridge, MA) were incubated for 2 h with PPP3 and digested PPP3 dissolved in DMEM/F12 medium containing 5% FBS, at 0.05 and 0.5 mg/mL. H_2O_2 was added at 1 mM, and cells were cultured for an additional 6 h. Culture supernatants were collected and stored at −80 °C for use in the IL-8 assays.

Table 2. Peptides Identified in PPP3 Digested with Pepsin and Pancreatin[a]

Position	Sequence	Observed mass, Da	Mr (expt), Da	Mr (calc), Da	Modification
1114-1121	FGTEPDAK	864.4256	863.4183	863.4025	
1115-1145	GTEPDAKTSSSSSSASSTATSSSSSSASSPN	1419.1215	2836.2285	2836.1966	
1115-1146	GTEPDAKTSSSSSSASSTATSSSSSSASSPNR	998.4506	2992.33	2992.2977	
1122-1146	TSSSSSSASSTATSSSSSSASSPNR	1148.0025	2293.9905	2293.9742	
1126-1138	SSSASSTATSSSS	933.6	1865.1854	1865.1653	9 Phospho (STY)
1128-1132	SASST	612.185	611.1777	611.1241	2 Phospho (STY)
1305-1319	EDDSSSSSSSSVLSK	751.3397	1500.6649	1500.6427	
1306-1317	DDSSSSSSSSVL	1157.4988	1156.4915	1156.4731	
1306-1319	DDSSSSSSSSVLSK	686.8148	1371.6151	1371.6001	
1306-1320	DDSSSSSSSSVLSKI	743.3641	1484.7137	1484.6842	
1306-1321	DDSSSSSSSSVLSKIW	836.4093	1670.8041	1670.7635	
1306-1322	DDSSSSSSSSVLSKIWG	864.9159	1727.8172	1727.785	

[a] The peptide preparation was dephosphorylated prior to LC-MS/MS. Observed m/z values are obtained by mass spectrometry. Mr(expt) is the uncharged molecular mass of the peptide, and Mr(calc) is the theoretical mass of the closest matching peptide.

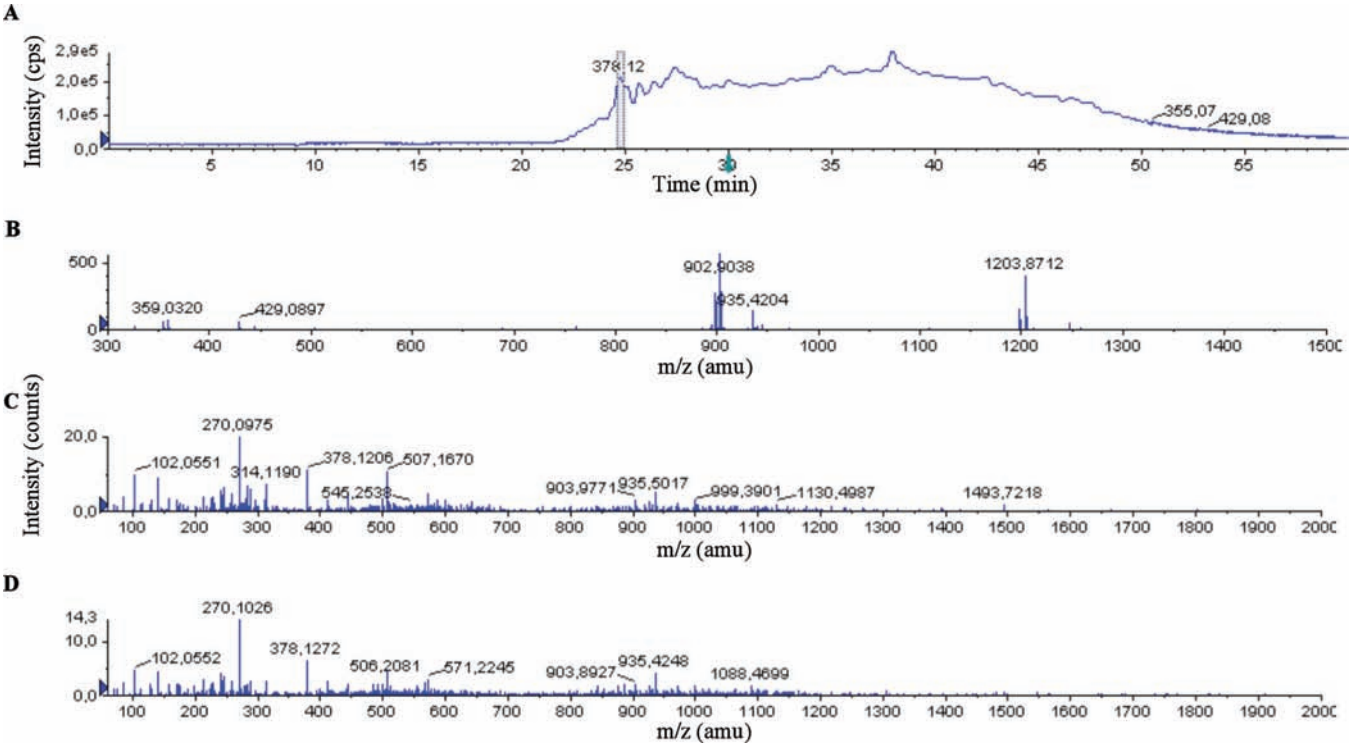

Figure 1. (A) Total ion chromatogram of the undigested PPP3 peptide, GTEPDAKTSSSSSSASSTATSSSSSSASSPNRKKPMD (positions 1115−1151). (B) Mass spectrum of a selected ion with m/z 378.12. Ions with (C) m/z 902.9038 and (D) m/z 1203.8712 were further fragmented, resulting in the respective MS/MS spectra. Peptides were detected by nanoelectrospray mass spectrometry coupled to a Q-TOF hybrid quadrupole/time-of-flight instrument and online liquid chromatography−tandem mass spectrometry.

Interleukin-8 Assay. To measure IL-8 concentrations in cell culture supernatants, 96-well microtiter plates were coated overnight at 4 °C with 0.05 μg/well mouse anti-human IL-8 antibody (BD Biosciences, San Diego, CA) in 100 mM sodium phosphate buffer (PBS), pH 9.0. Plates were blocked with PBS containing 1% (w/v) bovine serum albumin (BSA) (Thermo Fisher Scientific, Inc., Waltham, MA), followed by the addition of culture supernatants and IL-8 standards diluted in PBS containing 0.05% (v/v) Tween-20 (PBST; Thermo Fisher) and 1% BSA. Bound IL-8 was detected using biotinylated mouse anti-human IL-8 antibody (0.025 μg/well; BD Biosciences), followed by avidin-conjugated horseradish peroxidase (1:2000; BD Biosciences) diluted in PBST containing 1% BSA, and visualized using 3,3′,5,5′-tetramethylbenzidine (Sigma-Aldrich). The reaction was stopped using 1 M H_2SO_4, and the absorbance was read at 450 nm. IL-8 concentrations in the samples were determined from the IL-8 standard curve and expressed as picograms of IL-8 per milliliter of sample.

Influence of PPP3 on Antioxidant Gene Expression. Confluent Caco-2 cells were incubated in a 5% FBS-DMEM/F12 medium with 1 mg/mL of PPP3 for 2 h. H_2O_2 (1 mM) was added to the cells to induce oxidative stress for 1 h. At the end of 3 h, the cells were rinsed with PBS, and mRNA was extracted and synthesized into cDNA for RT-PCR.

Isolation of RNA and Reverse Transcription. Total RNA was extracted from adherent cultured cells using the Aurum Total RNA Mini Kit (Bio-Rad Laboratories). After the microtiter wells had been rinsed with PBS, lysis buffer (350 μL) was added to each well. Cell lysates

(200 μL) were transferred into new eppendorf tubes and mixed with equal volumes of 70% ethanol. The entire volume was transferred into the RNA binding column fitted into a 2 mL capless tube. The remaining steps were conducted in accordance with the manufacturer's instructions.

The quantity and quality of the RNA was verified by measuring the A_{260} and A_{280} (NanoDrop ND-1000; Thermo Scientific, Wilmington, DE) and by gel electrophoresis. First-strand cDNA was synthesized using the RT^2 First Strand Kit (SA Biosciences, Frederick, MD) according to the manufacturer's instructions.

Oxidative Stress and Antioxidant Defense PCR Array. The mRNA expression of a wide range of genes related to oxidative stress was quantified using RT-PCR with the RT^2 Profiler PCR Array: human oxidative stress and antioxidant defense. RT-PCR was carried out using the High Performance RT^2 qPCR Master Mixes (SA Biosciences) on a MyiQ Single Color Real-Time PCR Detection System (Bio-Rad Laboratories) using the following conditions: denaturation, 15 s at 95 °C; annealing, 15 s at 56 °C; and extension, 30 s at 72 °C.

Signaling Pathway Analysis. Fold up- or down-regulation was calculated relative to untreated control cells, and a gene was considered to be differentially expressed when it had a fold change of at least ±1.5. Gene ontology (GO) analysis was carried out using GoMiner.[12] A GO biological process was considered to be enriched when the Fisher's exact p value was ≤0.05. Functional pathway and network analyses were generated through the use of Ingenuity pathway analysis (version 2.0, Ingenuity Systems, Mountain View, CA). Ingenuity pathway analysis identified canonical pathways, biological processes, and gene interaction networks that were most significant to the gene expression data from the PCR array.

Statistical Analysis. All analyses were performed in triplicate unless specified otherwise. Statistical analyses were carried out using GraphPad (San Diego, CA) software. The statistical significance was determined by the Student's t test with a $P \leq 0.05$ taken as significant. Groups were considered to be statistically significant when $P \leq 0.05$. Results are reported as the mean ± SEM.

RESULTS AND DISCUSSION

Antioxidants have been shown to alleviate and suppress chronic intestinal diseases such as cancer and inflammatory bowel disease in vivo.[13−15] The GI tract is susceptible to ingested food compounds such as transition metal ions, heme, isoprostanes, additives, and lipids and their oxidized products.[16] These components act as oxidants, contributing to the ROS burden from endogenous and exogenous sources. Antioxidative stress compounds such as egg yolk-derived phosvitin phosphopeptides (PPP3)[7] may prevent the establishment of intestinal disease because they contribute to the up-regulation of endogenous antioxidant enzymes and glutathione synthesis in the epithelium.

Bioactive peptides in PPP3 were identified and were compared with PPP3 peptides after simulated gastrointestinal digestion. All peptides were identified as originating from the parent phosvitin region of vitellogenin II (UniProtKB/Swiss-Prot P02845, VIT2_CHICK), confirming the purity of the starting material for the phosphopeptide preparation. The PPP3 sample consisted of 13 identified peptides of 8−43 amino acid residues (Table 1), whereas digested PPP3 was made up of peptide fragments with 5−32 amino acids (Table 2). Three major PPP3 peptides emerged with the other 10 remaining peptides consisting of shorter fragments within these major sequences: GTEPDAKTSSSSSSASSTATSSSSSSASSPNRKKPMDE (PV residues 4−41); NSKSSSSSSKSSSSSSRSRSSSKSSSSSSSSSSSSSSKSSSSR (PV residues 155−197); and EDDSSSSSSSSVLSKIWGRHEIYQ (PV residues 244−257). The total ion chromatogram and an example of fragmentation spectra of a PPP3 peptide fragment (positions 1115−1151) are shown in Figure 1; other PPP3 peptides were identified in the same manner. Many pepsin- and pancreatin-digested peptide fragments were found within the PPP3 peptide sequence such as the 5 digested peptides within PPP3 (PV residues 4−41) and 6 digested peptides within PPP3 (PV residues 244−257). Unfortunately, digested fragments from PV 155−197 residues were not detected. Although these sequences were not identified in PPP3, it is likely due to difficulties in ionization rather than the absence of the peptide in the mixture due to highly monophosphorylated serine residues.

The substrate specificities of the digestive enzymes and the amino acid sequence of the original PPP3 preparation influence the size and sequence of digested peptides. Hydrolysis with pepsin generates peptides containing Y, F, or L in the N-terminal positions.[17] After pepsin digestion in the stomach, a mixture of

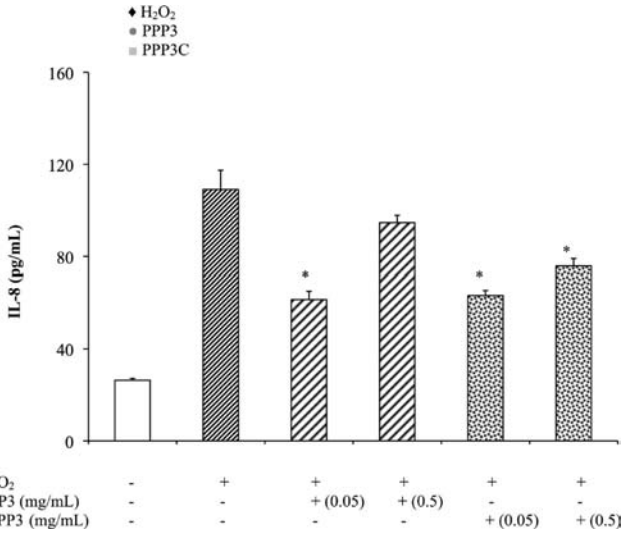

Figure 2. Effect of PPP3 and digested PPP3 (dPPP3) on IL-8 secretion in H_2O_2-treated Caco-2 cells. Cells were treated with 0.05 or 0.5 mg/mL of peptides for 2 h at 37 °C and then incubated with 1 mM H_2O_2 for 6 h. Data are presented as the mean ± SEM; $n = 3$. $P \leq 0.05$ compared to H_2O_2-treated cells.

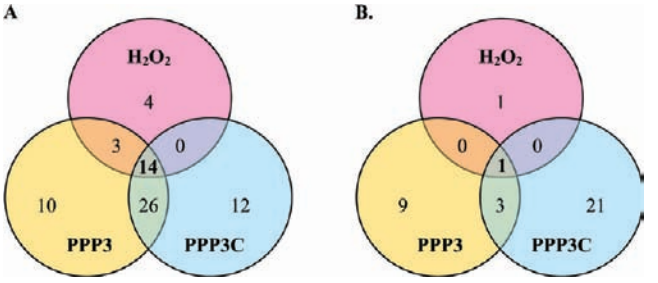

Figure 3. Differentially expressed genes and GO biological processes. (A) Genes were differentially expressed ($P \leq 0.05$) in H_2O_2, PPP3 followed by H_2O_2 (PPP3), and PPP3 alone (PPP3C). Cells were treated with 0.5 mg/mL of peptides for 2 h at 37 °C and then incubated with 1 mM H_2O_2 for 1 h. A total of 14 overlapping genes were commonly expressed among all three groups. (B) Gene ontology (GO) biological processes significantly enriched ($P \leq 0.05$) with the genes from H_2O_2, PPP3, and PPP3C treatments. Only one overlapping biological process was commonly enriched among all three groups.

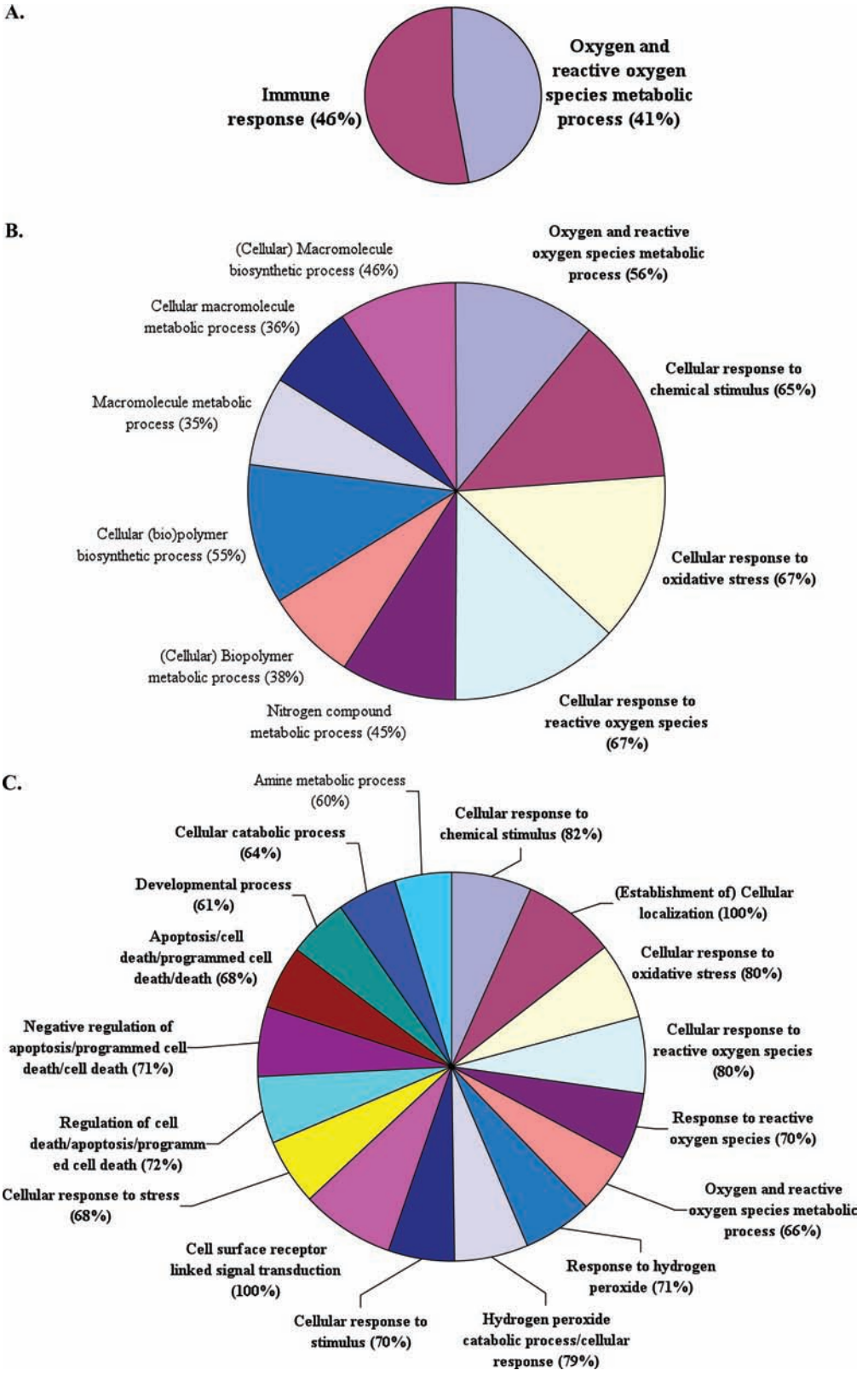

Figure 4. GO biological processes significantly ($P \leq 0.05$) enriched with genes from (A) H_2O_2, (B) PPP3, and (C) PPP3C groups. Up-regulated processes are highlighted in bold and downregulated processes are in lightface text.

pancreatic peptidases in the small intestine further cleaves oligopeptides into smaller fragments. Pancreatin is composed of the endopeptidases trypsin, α-chymotrypsin, and elastase and the exopeptidases carboxypeptidases A and B, with trypsin and chymotrypsin predominantly responsible for the majority of digestion in the duodenum. Because trypsin cleaves at the

carboxyl side of arginine or lysine[18,19] and PPP3 is prepared from the tryptic hydrolysis of phosvitin, peptides NSKSSSSSSK-SSSSSSRSRSSSKSSSSSSSSSSSSSSKSSSSR and EDDSSSSSS-SSVLSKIWGRHEIYQ are generated. Further tryptic digestion of PPP3 resulted in the identification of additional peptides of which two and three peptides have C-terminal arginine and lysine, respectively. Interestingly, when the GI-digested PPP3 sequences are compared with that of PPP3 and native phosvitin, tryptic hydrolysis occurs after amino acids that are not directly adjacent to contiguous serines. The steric hindrance created by the contiguous phosphorylated serines and the anionic character of the phosphate moieties likely conferred a marked resistance to the action of digestive enzymes.

Oligopeptides are capable of crossing the intestinal barrier and entering the bloodstream,[20,21] but post-translational modifications such as phosphorylation can affect peptide transport. Phosphopeptides have poor cell penetration because the negatively charged phosphate moieties are poorly transported across the cell membrane.[22] Even after simulated physiological digestion, digested PPP3, like pepsin- and pancreatin-digested casein phosphopepitdes (CPP), retain a high degree of phosphorylation.[23] Therefore, it is likely that these phosphorylated peptides exert bioactivity in the gut lumen or through receptors on the intestinal epithelial cells.[11] Using Caco-2 human epithelial cells, we demonstrated that both undigested and digested PPP3 at 0.05 mg/mL and at 0.05 and 0.5 mg/mL, respectively, significantly reduced the H_2O_2-stimulated secretion of IL-8 (Figure 2). It is therefore plausible that after PPP3 consumption, digested PPP3 contributes to the reduction of oxidative stress in the epithelium.

Contiguous serine and phosphoserine sequences are prevalent in the identified PPP3 peptides and may influence bioactivity. The majority of PPP3 peptides possess at least two contiguous serines, and Ser−Ser was found in all digested peptides. About 96% of seryl residues in phosvitin are phosphorylated,[24] and phosphorylated peptides were identified in both PPP3 and digested PPP3 preparations (Tables 1 and 2). The CPP sequence, SerP−SerP−SerP−Glu−Glu, is believed to present a polar, acidic region ideal for sequestering ferrous ion and quenching free radicals.[25] Although this effect is largely attributed to the phosphate groups in the phosphorylated serine residues, free phosphate and phosphoserine have a lower effect against oxidation compared to phosphorylated caseins.[26] Phosvitin phosphopeptides also have strong antioxidant capacities,[27] but whereas PPP3 influenced GSH and antioxidant enzyme pathways, serine and *o*-phosphoserine did not affect antioxidative stress activity.[7] These results suggest that contiguous phosphoserine sequences may interact with apical cell surface receptors and signal the enhancement of detoxification and antioxidant enzymes.

Gene ontology (GO) analysis was used to determine the biological roles and molecular functions of the differentially expressed genes in Caco-2 cells pretreated with PPP3 and stimulated with H_2O_2. Fold up- or down-regulation was calculated relative to untreated control cells, and expression was considered to be biologically significant if a fold change of 1.5 or greater was observed. Of the biologically significant up-/down-regulated genes observed, a total of 21 genes were differentially expressed in H_2O_2-stressed cells with 20 genes up-regulated and 1 gene down-regulated (Figure 3A) and corresponded to 2 up-regulated GO biological processes (Figure 3B): immune response [GO:0006955] and oxygen and reactive oxygen species metabolic process [GO:0006800] (Figure 4A). PPP3-treated oxidatively stressed cells revealed 53 differentially expressed genes with 35 genes up-regulated and 18 genes down-regulated. Thirteen GO processes were significantly enriched, with 4 biological processes up-regulated: oxygen and ROS metabolic process [GO:0006800], cellular response to chemical stimulus [GO:-0070887], cellular response to oxidative stress [GO:0034599], and cellular response to ROS [GO:0034614]. Down-regulated GO processes were related to cellular metabolic processes (Figure 4B). Although PPP3 control cells were not exposed to oxidant, 52 genes were differentially expressed, with 40 up-regulated and 12 down-regulated genes that comprised 25 up-regulated and 1 down-regulated GO biological process. Similar to the 4 up-regulated processes in PPP3, PPPC also up-regulated responses to ROS [GO:0000302] and hydrogen peroxide

Table 3. Gene Ontology (GO) Biological Processes Commonly Enriched with Genes Differentially Expressed in Caco-2 Cells in Response to H_2O_2 Stimulation, PPP3 Pretreatment and H_2O_2 Stimulation, and PPP3 Alone (PPP3C)[a]

	H_2O_2		PPP3		PPP3C	
GO process	genes	*P* value	genes	*P* value	genes	*P* value
oxygen and reactive oxygen species metabolic process [GO:0006800]	*PREX1*, NOX5, *NCF1*, LPO, EPX, EPHX2, *PRG3*, *PXDNL*, NOS2, MPO, DUOX2, PXDN, NCF2 (**13**/**32**)	0.005	**GPX3**, NOX5, **PRDX3**, **SOD2**, NCF1, LPO, EPX, EPHX2, **BNIP3**, **SFTPD**, **TPO**, **PRDX1**, NOS2, MPO, DUOX2, **AOX1**, PXDN, NCF2 (**18**/**32**)	0.03	**GPX3**, **DUOX1**, NOX5, **PRDX3**, **SOD2**, NCF1, **ALOX12**, LPO, **CCS**, EPX, **GPX4**, **BNIP3**, **SFTPD**, **TPO**, **PRDX1**, NOS2, MPO, DUOX2, **AOX1**, PXDN, NCF2 (**21**/**32**)	0.009

[a] Numbers in parentheses after the gene listing indicate the number of up-regulated genes relative to the total number of genes in the category. Genes in bold text indicate genes differentially expressed in PPP3 and PPP3C treatments that are absent during H_2O_2 stimulation alone. Italicized genes are unique to H_2O_2-stressed cells within the GO biological process. Genes are abbreviated as follows: ALOX12, arachidonate 12-lipoxygenase; AOX1, aldehyde oxidase 1; BNIP3, BCL2/adenovirus E1B 19 kDa interacting protein 3; CCS, copper chaperone for superoxide dismutase; DUOX1, dual oxidase 1; DUOX2, dual oxidase 2; EPHX2, epoxide hydrolase 2, cytoplasmic; EPX, eosinophil peroxidase; GPX3, glutathione peroxidase 3 (plasma); GPX4, glutathione peroxidase 4 (phospholipid hydroperoxidase); LPO, lactoperoxidase; MPO, myeloperoxidase; NCF1, neutrophil cytosolic factor 1; NCF2, neutrophil cytosolic factor 2; NOS2, nitric oxide synthase 2, inducible; NOX5, NADPH oxidase, EF-hand calcium binding domain 5; PRDX1, peroxiredoxin 1; PRDX3, peroxiredoxin 3; PREX1, phosphatidylinositol-3,4,5-trisphophate-dependent Rac; PRG3, proteoglycan 3; PXDN, peroxidasin homologue (*Drosophila*); PXDNL, peroxidasin homolog (*Drosophila*)-like; SFTPD, surfactant protein D; SOD2, superoxide dismutase 2; and TPO, thyroid peroxidase.

Table 4. Gene Ontology (GO) Biological Processes Commonly Enriched with Genes Differentially Expressed in Caco-2 Cells in Response to PPP3 Pretreatment and H_2O_2 Stimulation and PPP3 Alone (PPP3C)[a]

	PPP3		PPP3C	
GO process	genes	*P* value	genes	*P* value
cellular response to chemical stimulus [GO:0070887]	SFTPD, GPX3, PRDX5, TPO, PRDX1, PRDX3, DUOX2, LPO, MPO, PXDN, EPX (**11/17**)	0.03	GPX3, **DUOX1**, PRDX3, LPO, EPX, **GPX4**, SFTPD, PRDX5, TPO, **SELS**, PRDX1, MPO, DUOX2, PXDN (**14/17**)	0.001
cellular response to oxidative stress [GO:0034599]	GPX3, PRDX5, TPO, PRDX1, PRDX3, DUOX2, LPO, MPO, PXDN, EPX (**10/15**)	0.03	GPX3, PRDX5, **DUOX1**, TPO, PRDX1, PRDX3, DUOX2, LPO, MPO, PXDN, EPX, **GPX4(12/15)**	0.005
cellular response to reactive oxygen species [GO:0034614]	GPX3, PRDX5, TPO, PRDX1, PRDX3, DUOX2, LPO, MPO, PXDN, EPX (**10/15**)	0.03	GPX3, PRDX5, **DUOX1**, TPO, PRDX1, PRDX3, DUOX2, LPO, MPO, PXDN, EPX, **GPX4(12/15)**	0.005

[a] Numbers in parentheses after the gene listing indicate the number of up-regulated genes relative to the total number of genes in the category. Genes in bold text indicate genes differentially expressed in PPP3 control cells that are absent during PPP3-treated and H_2O_2-stimulated cells. Genes are abbreviated as follows: DUOX1, dual oxidase 1; DUOX2, dual oxidase 2; EPX, eosinophil peroxidase; GPX3, glutathione peroxidase 3 (plasma); GPX4, glutathione peroxidase 4 (phospholipid hydroperoxidase); LPO, lactoperoxidase; MPO, myeloperoxidase; PRDX1, peroxiredoxin 1; PRDX3, peroxiredoxin 3; PRDX5, peroxiredoxin 5; PXDN, peroxidasin homolog (*Drosophila*); SELS, selenoprotein S; SFTPD, surfactant protein D; SOD2, superoxide dismutase 2; and TPO, thyroid peroxidase.

Table 5. Biologically Significant Up- and Down-regulated Genes Related to Oxygen and Reactive Oxygen Species (ROS) Metabolism and Cellular Responses to Chemical Stimulus, Oxidative Stress, and ROS[a]

			fold change		
gene symbol	accession no.	gene description	H_2O_2	PPP3	PPP3C
ALOX12	NM_000697	arachidonate 12-lipoxygenase	1.09	1.33	**3.35**
AOX1	NM_001159	aldehyde oxidase 1	1.33	**2.90**	**3.18**
BNIP3	NM_004052	BCL2/adenovirus E1B 19 kDa interacting protein 3	1.01	**1.76**	**2.82**
CCS	NM_005125	copper chaperone for superoxide dismutase	1.13	1.10	**1.56**
DUOX1	NM_175940	dual oxidase 1	1.38	1.01	**1.82**
DUOX2	NM_014080	dual oxidase 2	**1.51**	**3.48**	**4.33**
EPHX2	NM_001979	epoxide hydrolase 2, cytoplasmic	**2.38**	**2.33**	1.13
EPX	NM_000502	eosinophil peroxidase	**3.23**	**4.14**	**3.98**
GPX3	NM_002084	glutathione peroxidase 3 (plasma)	1.12	**2.05**	**2.13**
GPX4	NM_002085	glutathione peroxidase 4 (phospholipid hydroperoxidase)	−1.02	1.32	**1.56**
LPO	NM_006151	lactoperoxidase	**15.70**	**19.89**	**4.32**
MPO	NM_000250	myeloperoxidase	**8.33**	**16.44**	**27.59**
NCF1	NM_000265	neutrophil cytosolic factor 1	**3.45**	**4.96**	**4.57**
NCF2	NM_000433	neutrophil cytosolic factor 2	**2.38**	**3.52**	**3.73**
NOS2	NM_000625	nitric oxide synthase 2, inducible	**3.29**	**9.38**	**10.49**
NOX5	NM_024505	NADPH oxidase, EF-hand calcium binding domain 5	**2.86**	**3.05**	**3.73**
PRDX1	NM_002574	peroxiredoxin 1	1.19	**1.58**	**1.51**
PRDX3	NM_006793	peroxiredoxin 3	1.35	**4.40**	**3.60**
PRDX5	NM_181652	peroxiredoxin 5	−1.14	**1.59**	**1.66**
PREX1	NM_020820	phosphatidylinositol-3.4,5-trisphophate-dependent Rac	**3.82**	−1.17	1.19
PRG3	NM_006093	proteoglycan 3	**2.22**	−3.63	−1.63
PXDN	NM_012293	peroxidasin homologue (*Drosophila*)	**2.76**	**6.45**	**4.65**
PXDNL	NM_144651	peroxidasin homologue (*Drosophila*)-like	**5.14**	−1.06	1.00
SELS	NM_203472	selenoprotein S	−1.19	1.33	**1.76**
SFTPD	NM_003019	surfactant protein D	1.09	**2.81**	**1.56**
SOD2	NM_000636	superoxide dismutase 2	1.14	**1.94**	**2.14**
TPO	NM_000547	thyroid peroxidase	1.34	**2.05**	**2.28**

[a] Genes are annotated using GenBank accession numbers. Fold change values ≥ +1.5 or ≤ −1.5 were chosen as cutoff values, defining increased and decreased expression, respectively. Up-regulated fold change values are highlighted in bold.

[GO:0042542 and GO:0042744], cellular response to stimulus [GO:0051716] and stress [GO:0033554], cell surface receptor linked signal transduction [GO:0007166], and general cellular localization, cell death, and catabolic and developmental processes (Figure 4C), with the exception of the amine metabolic process [GO:0009308], which was the only GO down-regulated process. These analyses indicate a strong response to oxygen and ROS, and indeed, this metabolic process [GO:0006800] was the most significant overlapping enriched GO biological process among the three treatments. Responses to oxidants, ROS, and chemical stimulus were even more enhanced in PPP3 and PPP3-treated without H_2O_2 (PPP3C) groups, suggesting PPP3 may play a major role in the detoxification of H_2O_2 via attachment to cell surface receptors. In the absence of oxidant, PPP3C cells also influenced apoptosis and cellular death biological processes; however, as both negatively [GO:0043066; GO:0043069; and GO:0060548] and positively [GO:0010941; GO:0042981; and GO:0043067] regulated processes were enriched, this may be indicative of cellular homeostasis maintenance.

The differentially expressed genes uniquely associated with H_2O_2 stimulation included PREX1 (phosphatidylinositol-3,4,5-triphosphate-dependent Rac), NCF1 (neutrophil cytolsolic factor-1), PRG3 (proteoglycan-3), and PXDNL (peroxidasin-like protein precursor) (Table 3). Both NCF1 and PRG3 are

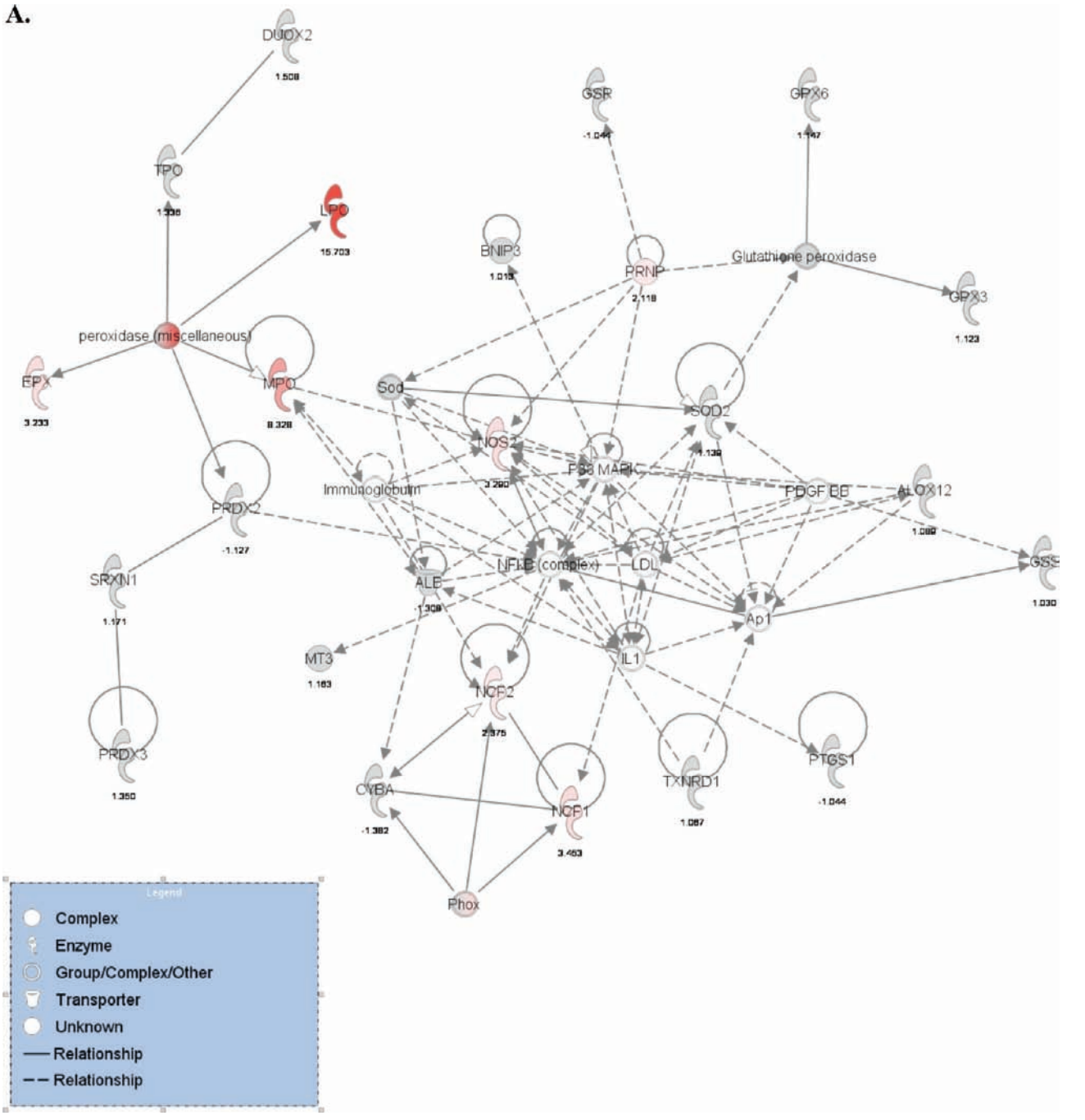

Figure 5. Continued

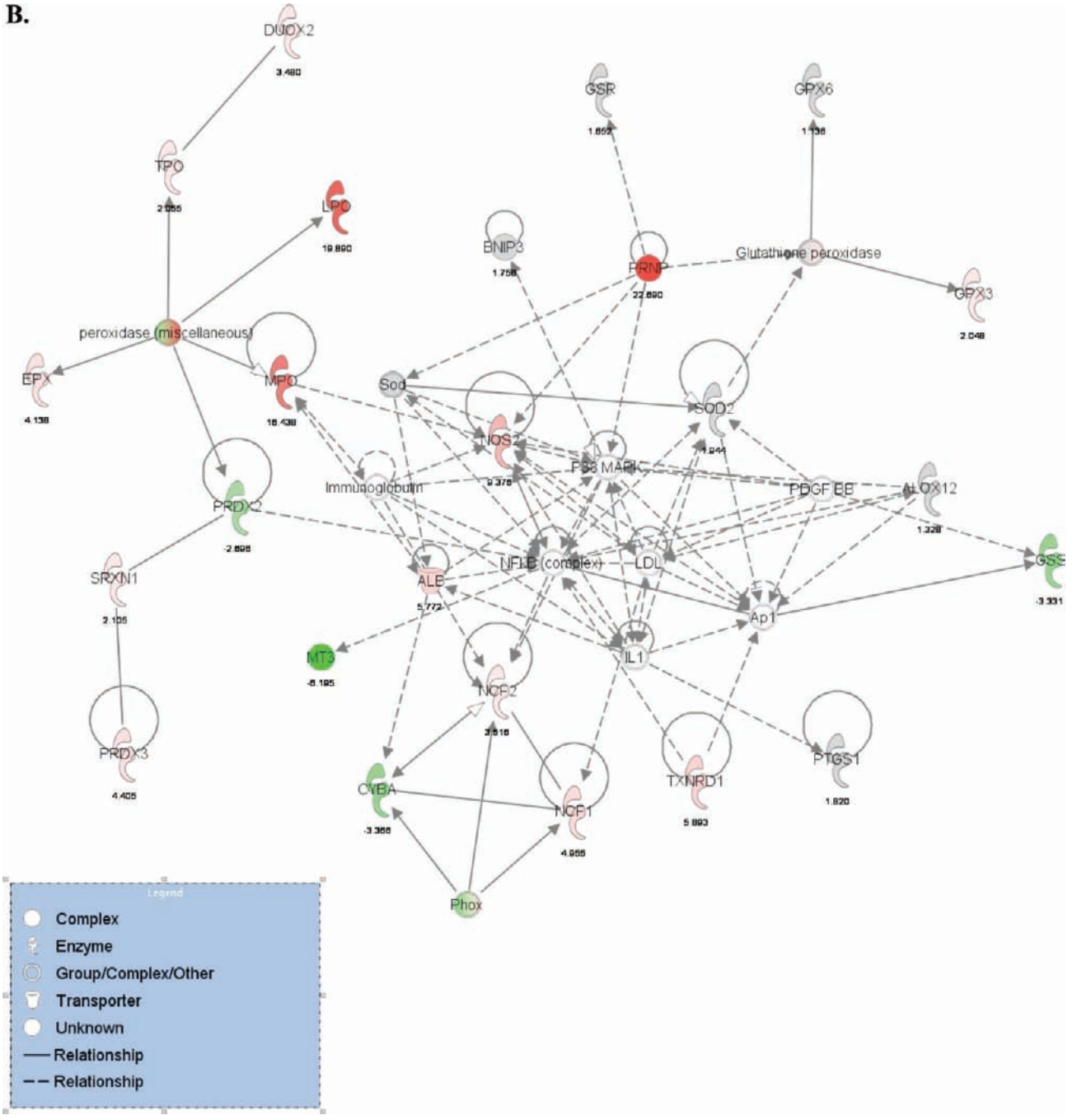

Figure 5. Continued

associated with superoxide production,[28,29] PREX1 functions in superoxide metabolism,[30] and PXDNL plays a role in phagocytosis and defense.[31] ROS production and immune defense are closely linked, and the up-regulated CCL5 (chemotactic cytokine), which recruits T cells, eosinophils, basophils, and leukocytes to inflammation sites,[32] within the enriched GO process [GO:0006955] is indicative of this. In comparison, PPP3 and PPP3C also influenced genes primarily involved in H_2O_2 and ROS detoxification such as GPX3, peroxiredoxin (PRDX1 and PRDX3), and SOD2, as well as a gene encoding a surfactant protein, SFTPD, which traps microorganisms and prevents oxidative stress and inflammation (Table 4).[33] The three other up-regulated genes, BNIP3, TPO, and AOX1, play roles in apoptosis, thryroid gland function, and oxidant formation, respectively.[34−36] PPP3 administered to cells in the absence of H_2O_2 also increased the expression of DUOX1, ALOX12, CCS, GPX4, and SELS in the GO processes associated with oxygen and ROS metabolism and in cellular responses to chemical stimulus, oxidative stress, and ROS (Table 5). Whereas dual oxidase 1 (DUOX1) and arachidonate 12-lipoxygenase (ALOX12) are associated with the production of ROS and inflammation,[37,38] respectively, the copper chaperone for superoxide dismutase (CCS) and GPX4 have antioxidant functions.[39] Selenoprotein S (SELS) may also play a role in regulating

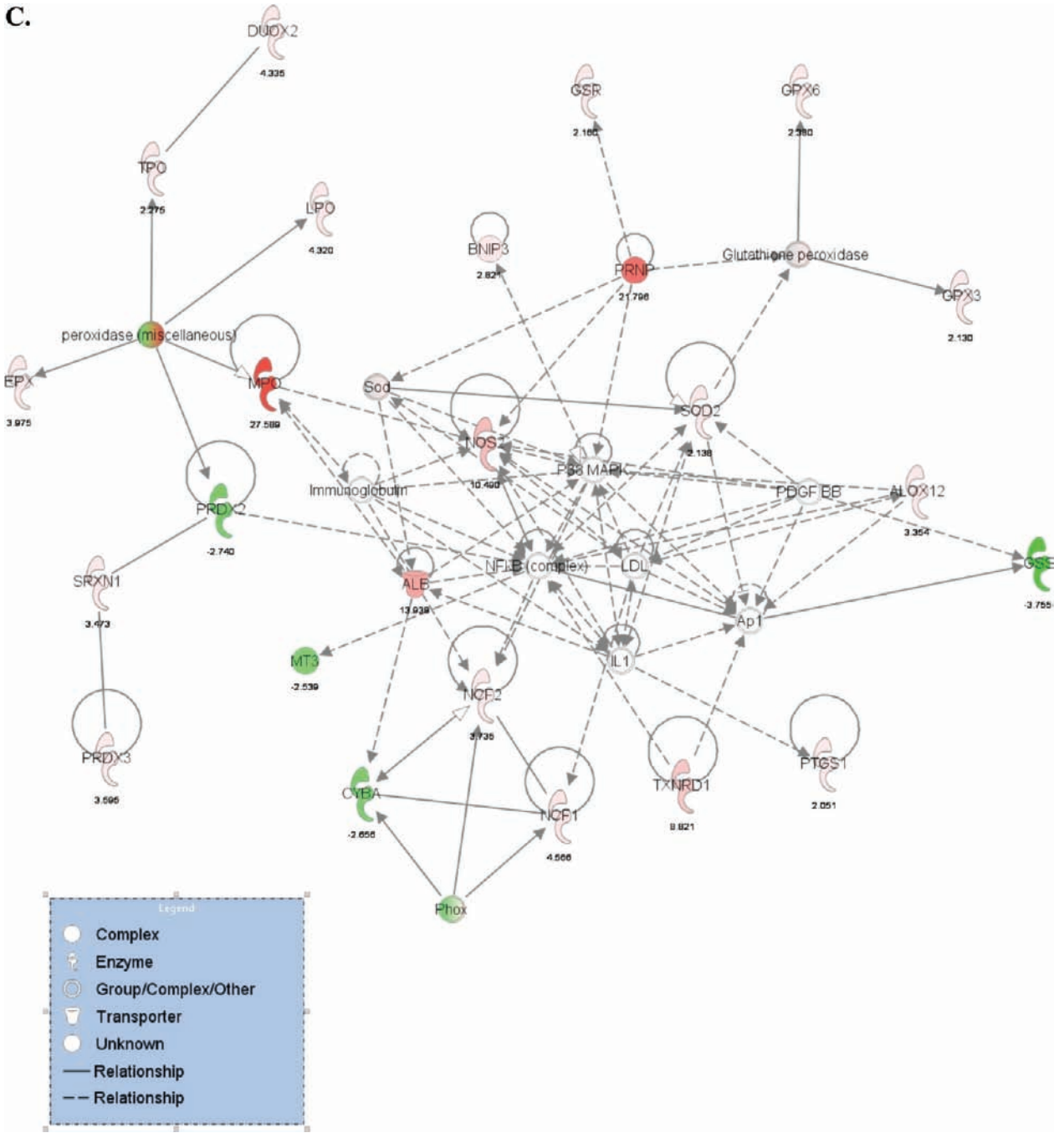

Figure 5. Pathway analysis of mRNA differentially expressed in (A) H_2O_2, (B) PPP3, and (C) PPP3C groups compared with baseline Caco-2 cells. Cells were treated with 0.5 mg/mL of peptides for 2 h at 37 °C and then incubated with 1 mM H_2O_2 for 1 h. PCR array fold change results were input into the Ingenuity pathway analysis program, which mapped genes to a network with NFκB as the main node. Numbers under the network shapes indicate the associated fold change. Color shading corresponds to the type of deregulation: red for up-regulated genes and green for down-regulated genes. The color intensity reflects the degree of up- or down-regulation. White open nodes are not from among the PCR array gene list, but are proteins associated with the regulation of some of these identified genes. Continuous and discontinuous lines represent direct and indirect functional and physical interaction between genes from the literature.

cytokine production,[40] suggesting that even PPP3 alone can have a profound influence in bolstering endogenous antioxidative defenses and preventing the development of inflammation.

Network analyses showed that the PPP3 antioxidant up-regulated pathways indirectly centered on the transcription factor, NFκB (Figure 5), which regulates genes related to immune function, inflammation, apoptosis, and cell proliferation.[41] Oxidants such as H_2O_2 can activate NFκB by phosphorylating inhibitor κB (IκB), releasing NFκB from the cytoplasm, and allowing its subsequent translocation into the nucleus where the transcription factor binds to and activates sequence-specific regions of DNA. It has been suggested that there is cross-talk between the

NFκB and Nrf2-ARE pathway, and several phytochemicals have been shown to suppress NFκB signaling while activating the antioxidative pathway.[42,43] It is likely that PPP3 also function in a similar manner, culminating in reduced IL-8 secretion, as seen in vitro, and in up-regulated antioxidant genes such as GPX3, PRDX3, and SOD2 (Figure 5B,C).

In conclusion, most of the peptides generated after PPP3 digestion in simulated GI are derived from the sequences identified in undigested PPP3. Digested PPP3 have antioxidative stress properties, and given the polyanionic nature of the peptides, they are likely retained in the gastrointestinal lumen, where they up-regulate antioxidative genes to prevent oxidative stress and promote gut health.

AUTHOR INFORMATION

Corresponding Author

*Phone: (519) 824-4120, ext. 52901. Fax: (519) 824-6631. E-mail: ymine@uoguelph.ca.

ACKNOWLEDGMENT

We thank the Advanced Foods and Materials Network (AFMNet), part of the Networks of Centres of Excellence (NCE), Canada for financially supporting this project.

ABBREVIATIONS USED

PPP3, phosvitin phosphopeptides; ROS, reactive oxygen species; GSH, glutathione; CAT, catalase; SOD, superoxide dismutase; GPx, glutathione peroxidase; GR, glutathione reductase; GST, glutathione-*S*-transferase; γ-GCS, γ-glutamylcysteine synthetase; Nrf2-ARE, nuclear response factor 2—antioxidant response element; IL-8, interleukin-8; H_2O_2, hydrogen peroxide; GI, gastrointestinal; FBS, fetal bovine serum; PBS, sodium phosphate buffer; BSA, bovine serum albumin; CPP, casein phosphopeptides; dPPP3, PPP3 digested with pepsin and pancreatin; LC, liquid chromatography; MS, mass spectrometry; NFκB, nuclear factor κB; IκB, inhibitor κB.

REFERENCES

(1) Cao, W.; Vrees, M. D.; Kirber, M. T.; Fiocchi, C.; V.E. Pricolo, V. E. Hydrogen peroxide contributes to motor dysfunction in ulcerative colitis. *Am. J. Physiol. Gastrointest. Liver Physiol.* **2004**, *286*, G833–G843.

(2) Masella, R.; Vari, R.; D'Archivio, M.; Di Benedetto, R.; Matarrese, P.; Malorni, W.; Scazzocchio, B.; Giovannini, C. Extra virgin olive oil biophenols inhibit cell-mediated oxidation of LDL by increasing the mRNA transcription of glutathione-related enzymes. *J. Nutr.* **2004**, *134*, 785–791.

(3) Biswas, S. K.; McClure, D.; Jimenez, L. A.; Megson, I. L.; Rahman, I. Curcumin induces glutathione biosynthesis and inhibits NF-κB activation and interleukin-8 release in alveolar epithelial cells: mechanism of free radical scavenging activity. *Antioxid. Redox Signal.* **2005**, *7*, 32–41.

(4) Molina, M. F.; Sanchez-Reus, I.; Iglesias, I.; Benedi, J. Quercetin, a flavonoid antioxidant, prevents and protects against ethanol-induced oxidative stress in mouse liver. *Biol. Pharm. Bull.* **2003**, *26*, 1398–1402.

(5) Li, Y.; Cao, Z.; Zhu, H. Upregulation of endogenous antioxidants and phase 2 enzymes by the red wine polyphenol, resveratrol in cultured aortic smooth muscle cells leads to cytoprotection against oxidative and electrophilic stress. *Pharmacol. Res.* **2006**, *53*, 6–15.

(6) Griffith, O. W. Biologic and pharmacologic regulation of mammalian glutathione synthesis. *Free Radical Biol. Med.* **1999**, *27*, 922–935.

(7) Katayama, S.; Ishikawa, S.; Fan, M. Z.; Mine, Y. Oligophosphopeptides derived from egg yolk phosvitin up-regulate γ-glutamylcysteine synthetase and antioxidant enzymes against oxidative stress in Caco-2 cells. *J. Agric. Food Chem.* **2007**, *55*, 2829–2835.

(8) Katayama, S.; Xu, X.; Fan, M. Z.; Mine, Y. Antioxidative stress activity of oligophosphopeptides derived from hen egg yolk phosvitin in Caco-2 cells. *J. Agric. Food Chem.* **2006**, *54*, 773–778.

(9) Albright, K. J.; Gordon, D. T.; Cotterill, O. J. Release of iron from phosvitin by heat and food-additives. *J. Food Sci.* **1984**, *49*, 78–81.

(10) Byrne, B. M.; van het Schip, A. D.; van de Klundert, J. A.; Arnberg, A. C.; Gruber, M.; Ab, G. Amino acid sequence of phosvitin derived from the nucleotide sequence of part of the chicken vitellogenin gene. *Biochemistry* **1984**, *23*, 4275–4279.

(11) Shimizu, M.; Son, D. O. Food-derived peptides and intestinal functions. *Curr. Pharm. Des.* **2007**, *13*, 885–895.

(12) Zeeberg, B. R.; Feng, W.; Wang, G.; Wang, M. D.; Fojo, A. T.; Sunshine, M.; Narasimhan, S.; Kane, D. W.; Reinhold, W. C.; Lababidi, S.; Bussey, K. J.; Riss, J.; Barrett, J. C.; Weinstein, J. N. GoMiner: a resource for biological interpretation of genomic and proteomic data. *Genome Biol.* **2003**, *4*, R28.

(13) Yamane, T.; Nakatani, H.; Kikuoka, N.; Matsumoto, H.; Iwata, Y.; Kitao, Y.; Oya, K.; Takahashi, T. Inhibitory effects and toxicity of green tea polyphenols for gastrointestinal carcinogenesis. *Cancer* **1996**, *77*, 1662–1667.

(14) Mazzon, E.; Muia, C.; Paola, R. D.; Genovese, T.; Menegazzi, M.; De Sarro, A.; Suzuki, H.; Cuzzocrea, S. Green tea polyphenol extract attenuates colon injury induced by experimental colitis. *Free Radical Res.* **2005**, *39*, 1017–1025.

(15) Oz, H. S.; Chen, T. S.; McClain, C. J.; de Villiers, W. J. Antioxidants as novel therapy in a murine model of colitis. *J. Nutr. Biochem.* **2006**, *16*, 297–304.

(16) Halliwell, B.; Zhao, K.; Whiteman, M. The gastrointestinal tract: a major site of antioxidant action? *Free Radical Res.* **2000**, *33*, 819–830.

(17) Savoie, L.; Gauthier, S. F.; Marin, J.; Pouliot, Y. *In vitro* determination of the release kinetics of peptides and free amino acids during the digestion of food proteins. *J. AOAC Int.* **2005**, *88*, 935–948.

(18) Brown, W. E.; Wold, F. Alkyl isocyanates as active-site-specific reagents for serine proteases. Identification of the active-site serine as the site of reaction. *Biochemistry* **1973**, *12*, 835–840.

(19) Folk, J. E.; Schirmer, E. W. Chymotrypsin. Isolation of zymogen and active enzyme-preliminary structure and specificity studies. *J. Biol. Chem.* **1965**, *240*, 181.

(20) Chabance, B.; Marteau, P.; Rambaud, J. C.; Migliore-Samour, D.; Boynard, M.; Perrotin, P.; Guillet, R.; Jolles, P.; Fiat, A. M. Casein peptide release and passage to the blood in humans during digestion of milk or yogurt. *Biochimie* **1998**, *80*, 155–165.

(21) Roberts, P. R.; Burney, J. D.; Black, K. W.; Zaloga, G. P. Effect of chain length on absorption of biologically active peptides from the gastrointestinal tract. *Digestion* **1999**, *60*, 332–337.

(22) Richter, S.; Bergmann, R.; Pietzsch, J.; Ramenda, T.; Steinbach, J.; Wuest, F. Fluorine-18 labeling of phophopeptides: a potential approach for the evaluation of phosphopeptide metabolism in vivo. *Peptide Sci.* **2009**, *92*, 479–488.

(23) Miquel, E.; Gomez, J. A.; Alegria, A.; Barbera, R.; Farre, R.; Recio, I. Identification of casein phosphopeptides released after simulated digestion of milk-based infant formulas. *J. Agric. Food Chem.* **2005**, *53*, 3426–3433.

(24) Anton, M.; Castellani, O.; Guérin-Dubiard, C. Phosvitin. In *Bioactive Egg Compounds*; Springer-Verlag: Berlin, Germany, 2007; pp 17—24.

(25) Kitts, D. D. Antioxidant properties of casein-phosphopeptides. *Trends Food Sci. Technol.* **2005**, *16*, 549–554.

(26) Cervato, G.; Cazolla, R.; Cestaro, B. Studies on the antioxidant activity of milk. *Int. J. Food Sci. Nutr.* **1999**, *50*, 1557–1559.

(27) Xu, X.; Katayama, S.; Mine., Y. Antioxidant activity of tryptic digests of hen egg yolk phosvitin. *J. Food Agric. Sci.* **2007**, *87*, 2604–2608.

(28) Takeshita, F.; Ishii, K. J.; Kobiyama, K.; Kojima, Y.; Coban, C.; Sasaki, S.; Ishii, N.; Klinman, D. M.; Okuda, K.; Akira, S.; Suzuki, K. TRAF4 acts as a silencer in TLR-mediated signaling through the association with TRAF6 and TRIF. *Eur. J. Immunol.* **2005**, *35*, 2477–2485.

(29) Plager, D. A.; Loegering, D. A.; Weiler, D. A.; Checkel, J. L.; Wagner, J. M.; Clarke, N. J.; Naylor, S.; Page, S. M.; Thomas, L. L.; Akerblom, I.; Cocks, B.; Stuart, S.; Gleich, G. J. A novel and highly divergent homolog of human eosinophil granule major basic protein. *J. Biol. Chem.* **1999**, *274*, 14464–14473.

(30) Cronin, A.; Decker, M.; Arand, M. Mammalian soluble epoxide hydrolase is identical to liver hepoxilin hydrolase. *J. Lipid Res.* **2011**, *52*, 712–719.

(31) Nelson, R. E.; Fessler, L. I.; Takagi, Y.; Blumberg, B.; Keene, D. R.; Olson, P. F.; Parker, C. G.; Fessler, J. H. Peroxidasin: a novel enzyme-matrix protein of *Drosophila* development. *EMBO J.* **1994**, *13*, 3438–3447.

(32) Kabelitz, D.; Wesch, D. Features and functions of $\gamma\delta$T lymphocytes: focus on chemokines and their receptors. *Crit. Rev. Immunol.* **2003**, *23*, 339–370.

(33) Hartshorn, K. L.; White, M. R.; Rynkiewicz, M.; Sorensen, G.; Holmskov, U.; Head, J.; Crouch, E. C. Monoclonal antibody-assisted structure-function analysis of the carbohydrate recognition domain of surfactant protein D. *Am. J. Physiol. Lung Cell Mol. Physiol.* **2010**, *299*, L384–L392.

(34) Boyd, J. M.; Malstrom, S.; Subramanian, T.; Venkatesh, L. K.; Schaeper, U.; Elangovan, B.; D'Sa-Eipper, C.; Chinnadurai, G. Adenovirus E1B 19 kDa and Bcl-2 proteins interact with a common set of cellular proteins. *Cell* **1994**, *79*, 341–351.

(35) Kotani, T.; Umeki, K.; Kawano, J.; Suganuma, T.; Hishinuma, A.; Ieiri, T.; Harada, S. Partial iodide organification defect caused by a novel mutation of the thyroid peroxidase gene in three siblings. *Clin. Endocrinol. (Oxford)* **2003**, *59*, 198–206.

(36) Wright, R. M.; Riley, M. G.; Weigel, L. K.; Ginger, L. A.; Costantino, D. A.; McManaman, J. L. Activation of the human aldehyde oxidase (hAOX1) promoter by tandem cooperative Sp1/Sp3 binding sites: identification of complex architecture in the hAOX upstream DNA that includes a proximal promoter, distal activation sites, and a silencer element. *DNA Cell Biol.* **2000**, *19*, 459–474.

(37) Geiszt, M.; Witta, J.; Baffi, J.; Lekstrom, K.; Leto, T. L. Dual oxidases represent novel hydrogen peroxide sources supporting mucosal surface host defense. *FASEB J.* **2003**, *17*, 1502–1504.

(38) Kühn, H.; O'Donnell, V. B. Inflammation and immune regulation by 12/15-lipoxygenases. *Prog. Lipid Res.* **2006**, *45*, 334–356.

(39) Culotta, V. C.; Klomp, L. W.; Strain, J.; Casareno, R. L.; Krems, B.; Gitlin, J. D. The copper chaperone for superoxide dismutase. *J. Biol. Chem.* **1997**, *272*, 23469–23472.

(40) Zeng, J.; Du, S.; Zhou, J.; Huang, K. Role of SelS in lipopolysaccharide-induced inflammatory response in hepatoma HepG2 cells. *Arch. Biochem. Biophys.* **2008**, *478*, 1–6.

(41) Martindale, J. L.; Holbrook, N. J. Cellular response to oxidative stress: signaling for suicide and survival. *J. Cell. Physiol.* **2002**, *192*, 1–15.

(42) Gao, Z.; Chiao, P.; Zhang, X.; Zhang, X.; Lazar, M. A.; Seto, E.; Young, H. A.; Ye, J. Coactivators and corepressors of NF-κB in IκB α gene promoter. *J. Biol. Chem.* **2005**, *280*, 21091–21098.

(43) Li, W.; Khor, T. O.; Xu, C.; Shen, G.; Jeong, W. S.; Yu, S.; Kong, A. N. Activation of Nrf2-antioxidant signaling attenuates NFκB-inflammatory response and elicits apoptosis. *Biochem. Pharmacol.* **2008**, *76*, 1485–1489.